Chapter 2

Methodology

2.1 Introduction

This chapter deals with the methodology used for low cycle fatigue (LCF) analysis of as received aluminium alloy AA6063 and at different heat treatment temperatures and at different soaking times and AA6063/SiCp metal matrix composite (MMC) for cantilever specimen at room temperature condition and simply support specimen at room temperature condition. The methodologies adopted are experimental, theoretical, numerical and empirical. LCF analysis of simply support specimen is discussed which is performed experimentally.

2.2 Experimental procedure

2.2.1 Material and preparations

The material used for experimental study in this chapter is the as received aluminum alloy AA6063.The aluminium alloy AA6063 was procured from Hindalco Company, India. Aluminium Alloy rods of 15 mm diameter and plate 12mm × 12mm of various lengths are prepared for all the tests. These rods are then cut into small pieces in Machine shop and CISF (Central Instrumentation Service and Fabrication Laboratory) shops. Polishing of the surfaces of the samples is initially done by emery paper made of silicon carbide with different grades viz. P400, P600, P800, P1000 and P1500. The polishing was done with emery papers starting from coarse i. e. P400 and ending with fine i. e. P1500. Next, liquid alumina polishing is done with alumina solution and cloth obtained from Chennai Metco Pvt Ltd in Machine shop.

The cast AA6063-T6 alloy is reinforced with 2% and 8% by volume of SiC particles. The particle size of SiC particulate reinforcement is 400 mesh i.e. 37µm. Casting is performed in foundry shop of Department of Metallurgical Engineering, IIT(BHU) using Muffle Furnace Stirr casting type as shown in Fig. 2.1.

Fig. 2.1 Stirr cast type Muffle Furnace

2.3 Experiments

2.3.1 Chemical composition Test

Chemical composition test is performed using "Thermo Scientific ARL Optim: X-Ray Analyzer 166"as shown in Fig. 2.2, with supply voltage 230V-1.5 KV to understand the chemical composition of the specimen, in the Department of Chemical Engineering, IIT(BHU) .

Fig. 2.2 Chemical Composition Analyzer

2.3.2 EDAX-SEM test

Chemical composition is also studied through Energy Dispersive X-ray Analysis (EDAX) analysis.

Fig. 2.3 SEM - EDAX System

The quantitative analysis by EDAX is performed with a relatively high voltage of 10 KV to improve the contrast between metallic and matrix phases. Microstructural features and failure mechanisms are studied through scanning electron microscopy (SEM). The SEM-EDAX system used is FEG Quanta -200 as shown in Fig. 2.3, of the Department of Metallurgical Engineering, IIT (BHU).

2.3.3 Tensile test

Before fatigue test, the monotonic tensile test is performed with cylindrical Hounsfield tensile specimen with gauge length, 15.4 mm and gauge diameter 4.5 mm as shown in Fig. 2.4, at a nominal strain rate of $1.2 * 10^{-4}\ s^{-1}$ using Instron 4206 machine

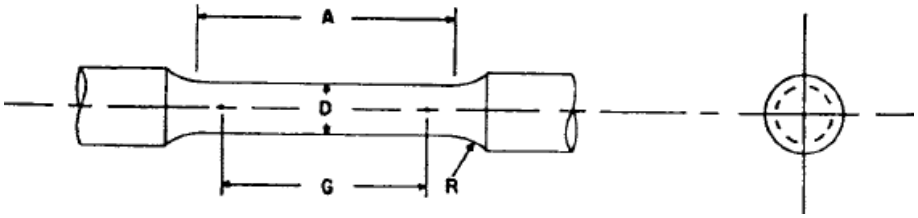

G= 20.00 ± 0.04, D=4.00 ± 0.05, R=4, A=24

Fig. 2.4 Tensile test specimen (All dimension are in mm)

having loading capacity of 100KN as shown in Fig. 2.5, in the Department of Metallurgical Engineering , IIT(BHU), using test methods specified by ASTM Standard B557M–10 [55] .

Fig. 2.5 Tensile Testing Machine

2.3.4 Torsion test

Torsion test is also performed with the sample as shown in Fig. 2.6 in the Department of Mechanical Engineering, IIT(BHU) using Torsion testing machine of Avery (7601 CHG), Birmingham, England having capacity 60000 kg.cm as shown in Fig. 2.7.

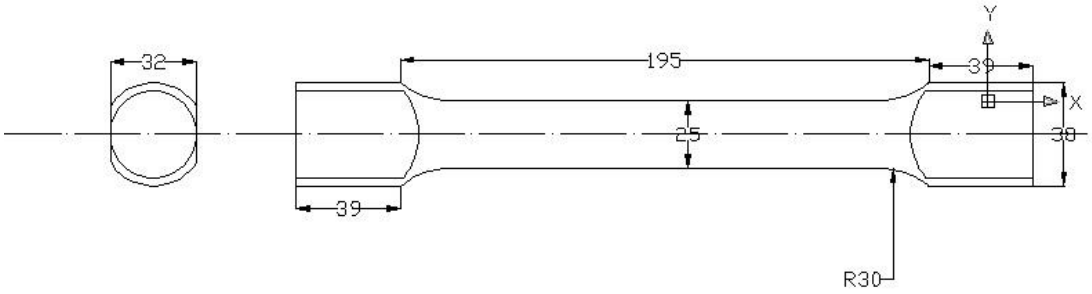

Fig. 2.6 Torsion test specimen (All dimension in mm)

Fig. 2.7 Torsion testing machine

2.3.5 Fatigue test

2.3.5.1 Cantilever beam specimen

Figure 2.8 shows the geometry of the cantilever specimen for rotating low cycle fatigue test with gage length 106 mm and gage diameter 8 mm. The test is done using WP 140 Fatigue Testing Apparatus, Gunt, Hamburg, Germany as shown in Fig. 2.9 in the Department of Mechanical Engineering , IIT(BHU) .

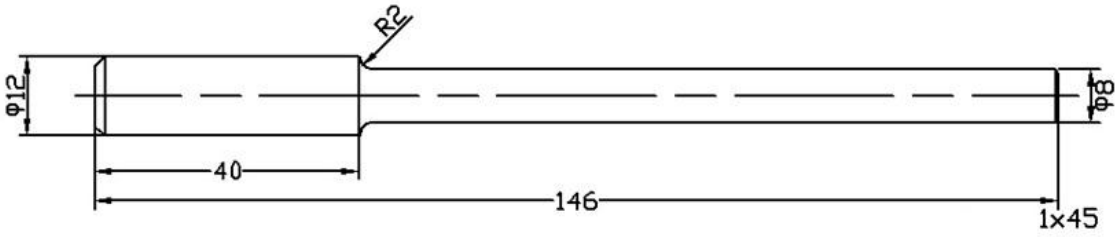

Fig. 2.8 Cantilever fatigue test specimen (All dimensions are in mm)

Fig. 2.9 Cantilever fatigue testing machine

2.3.5.2 Simply Support beam specimen

The geometry of simply support beam specimen for push-pull low cycle fatigue test of AA6063 are made of rod of 15 mm diameter as per the British standard (BS 12-1950) and shown in Fig.2.10. The simply support fatigue test were performed in a closed-loop servo-hydraulic, completely computer controlled axial load frame fatigue testing (Model No.= 810 MTS) machine having capacity of 50 kN as shown in Fig. 2.11 of Department of Metallurgical Engineering, IIT(BHU).

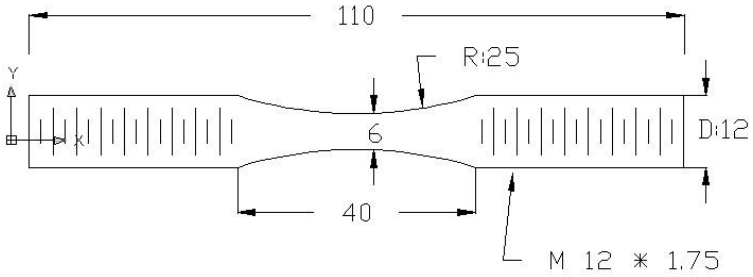

Fig. 2.100 Simply supported fatigue testing specimen (All dimensions are in mm)

Fig. 2.11 Simply support push-pull fatigue test system

2.3.6 X-RD test

X-ray Diffraction tests were performed using Rigaku-Mini Flex II Desktop-X-Ray Diffractometer as shown in Fig. 2.11. in the Department of Ceramic Engineering, IIT(BHU).

Fig. 2.11 X-Ray diffractometer

2.3.7 Optical micrograph test

Optical micrography is studied for fatigue test samples using metallux-3 optical microscope of Carl Zeiss Micro Imagine Gmb H 37081, Germany as shown in Fig. 2.12, of the Department of Metallurgical Engineering, IIT (BHU). The samples are prepared by etching with a solution containing HNO_3, HF and water in proportion of 5% , 10% and 85%, respectively by volume .

Fig. 2.12 Optical microscope

2.3.8 Hardness test

Micro hardness test is carried out using HMV-2 shimadzu micro hardness tester as shown in Fig. 2.13 in the Department of Metallurgical Engineering, IIT (BHU), of AA6063 alloy subjected to different applied loads.

Vickers micro hardness (HV) is measured on the plane surface with different loads. Prior to each hardness measurement, the surfaces of the specimen is polished mechanically using emery paper and alumina liquid to remove the surface reactions.

Fig. 2.13 Micro hardness test Instrument

Fig. 2.14 Vickers macro hardness (HV) testing machine

An average of at least three readings on the surface of the specimen are taken to obtain a micro hardness value. Vickers macro hardness (HV) test was done with different applied load using Vickers Macro Hardness testing machine of model MECH C.S/VM50, in the Department of Mechanical Engineering, IIT (BHU) as shown in Fig. 2.14.

2.4 Theoretical Analysis

2.4.1 Tensile Analysis

The strain hardness exponent (n) and strength coefficient (K) can be obtained from log-log plot of true plastic stress and true plastic strain. The slope of the plot gives (*n*) and intercept of the plot at unit plastic strain gives K based on the relation [3-5] as given below

$$\sigma = K\varepsilon_p^n \tag{2.1}$$

2.4.2 Low Cycle Fatigue (LCF) Analysis

The theoretical investigation of low cycle fatigue (LCF) is performed using the method elaborated by Fatemi et al. [40] and Eleiche et al. [41]. The adopted process for the present analysis is described as follows.

According to Basquin[1], the strain-life data can be linearized on log-log scale as

$$\frac{\Delta\varepsilon_e}{2} = \frac{\sigma_f^{'}}{E}\left(2N_f\right)^b \tag{2.2}$$

Coffin and Manson found that the plastic strain-life data could also be linearized on log–log scale as

$$\frac{\Delta\varepsilon_p}{2} = \varepsilon_f^{'}\left(2N_f\right)^c \tag{2.3}$$

The total strain amplitude can then be considered as the summation of elastic and plastic amplitudes and the resulting strain-life curve can be expressed as:

$$\varepsilon_a = \frac{\Delta\varepsilon_e}{2} + \frac{\Delta\varepsilon_p}{2} = \frac{\sigma_f^{'}}{E}\left(2N_f\right)^b + \varepsilon_f^{'}\left(2N_f\right)^c \tag{2.4}$$

Where $\sigma_f^{'}$ is the fatigue strength coefficient, b is the fatigue strength exponent, $\varepsilon_f^{'}$ is the fatigue ductility coefficient and c is the fatigue ductility exponent. The life at which

elastic and plastic components of strain are equal is called the transition fatigue life (2Nt). For lives shorter than 2Nt the deformation is mainly plastic. The cyclic strength coefficient, K', and the cyclic strain hardening exponent, n' can be estimated from the low-cycle fatigue parameters as follows [57] :

$$K' = \frac{\sigma_f'}{(\varepsilon_f')^{\frac{b}{c}}} \tag{2.5}$$

$$n' = \frac{b}{c} \tag{2.6}$$

The first step of theoretical analysis is determination of hysteresis angle. Figure 2.16 shows that all points e.g. A and B are at the same distance from the deflection axis $\alpha\alpha$ (strain axis). These points will have exactly the same strain and stress levels and consequently they have the same hysteresis loop. Note that the loading axis ZZ in this case coincides with the deflection axis $\alpha\alpha$. Figure 2.17*a* shows the same cross-section of the round specimen, now subjected to rotating bending with surface strain amplitude ε_s. The two elements A and B are at the same distance from the strain axis $\alpha\alpha$ (deflection axis). Therefore, the two elements are at the same strain level, ε as shown in Fig. 2.16*b*. On the other hand the two elements now share the same hysteresis loop also, but are not, at any given moment in line, at the same stress level, owing to rotation, as shown in Fig. 2.16*a*. Point A is moving towards a higher stress level, whereas point B, is moving towards a lower one. Each point will ultimately reach a maximum strain level ε_m, when they achieve the maximum vertical distance R from the strain axis. Because of rotation, the stress-strain relation for all points along a circle with radius *r* is represented by one hysteresis loop. Therefore the Section will deflect about the axis $\alpha\alpha$, which makes an

angle with the loading axis *ZZ*. This angle is designated as hysteresis angle (ϕ) to indicate the presence of hysteresis loops on the radius of the section. When the behaviour is elastic, as in high-cycle fatigue, the hysteresis loops degenerate to an elastic line, Therefore the hysteresis angle vanishes. In this case, the rotating bending problem can be treated as a flexural bending problem, where in the loading and strain axes always coincide. Considering low-cycle fatigue tests under rotating bending, a test specimen may be developed such that the tested zone has constant surface strain amplitude ε_s. Figure 2.17a shows the cross-section in the tested zone with outer radius ***R***, subjected to rotating bending.

Since in bending it is commonly assumed that plane sections remain plane, the strain will vary linearly across the section, as shown in Fig. 2.16*b*. The strain ε_m, at distance ***r*** from the deflection axis $\alpha\alpha$ (strain axis) is given as

$$\varepsilon_m = \left(\frac{r}{R}\right)\varepsilon_s \tag{2.7}$$

Points A and B, are at the same height from the deflection axis and rotate on the circle with radius *r*. Therefore the stress-strain relation of these points is represented by one hysteresis loop with strain amplitude ε_m, as shown in Fig. 2.16*c*. To obtain the value of stress at point A(σ_A) or at point B(σ_B), the shape of the hysteresis loop must first be defined. According to the Masing rule, the shape of the settled hysteresis loop branches can be obtained by magnifying the relation of the stress-strain curve by a factor of 2. The cyclic stress-strain curve is described by Ramberg Osgood relation and given as

$$\varepsilon = \left(\frac{\sigma}{E}\right) + \left(\frac{\sigma}{K'}\right)^{\frac{1}{n'}} \tag{2.8}$$

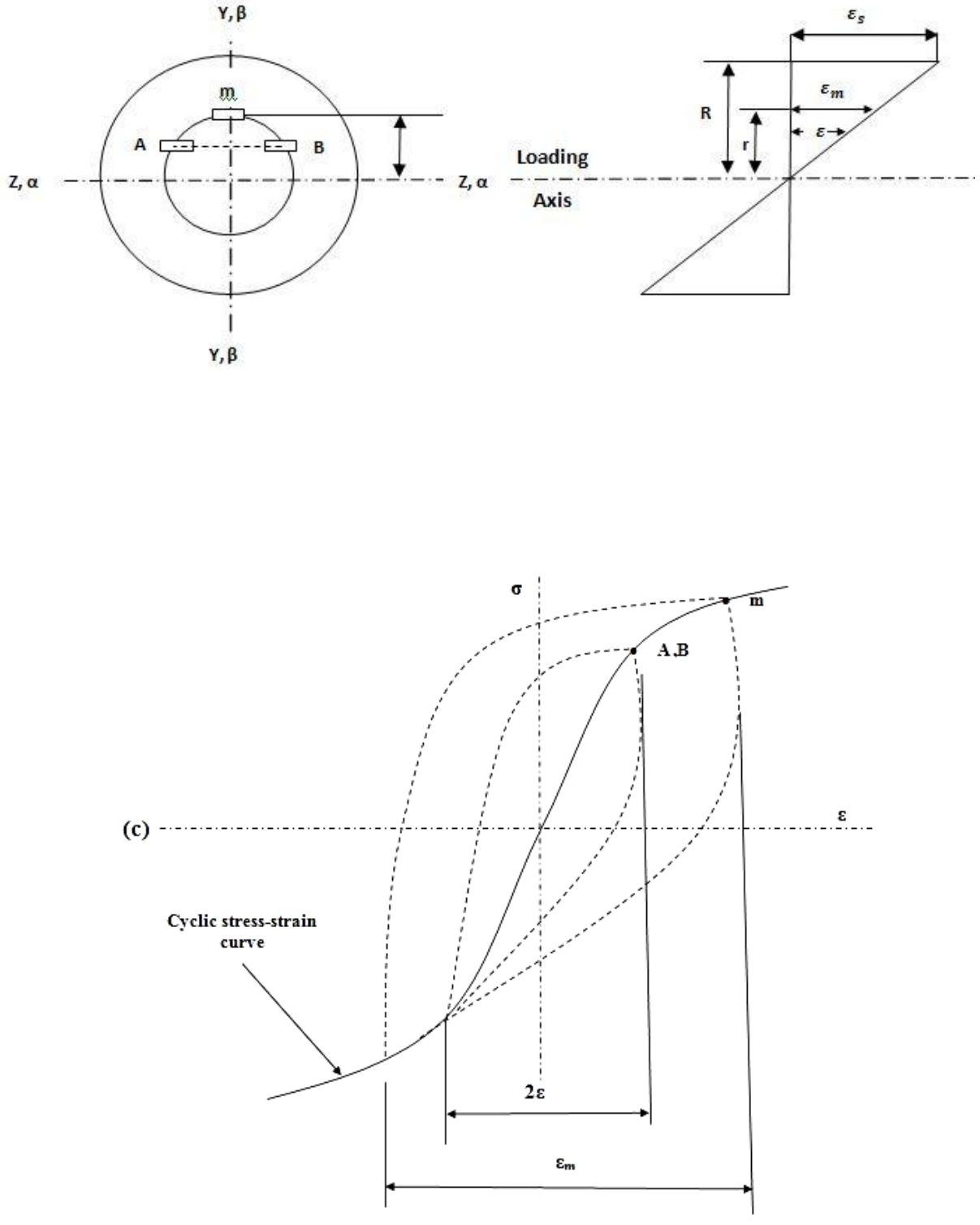

Fig. 2.15 Stress distribution in flexural bending from axial strain cyclic properties

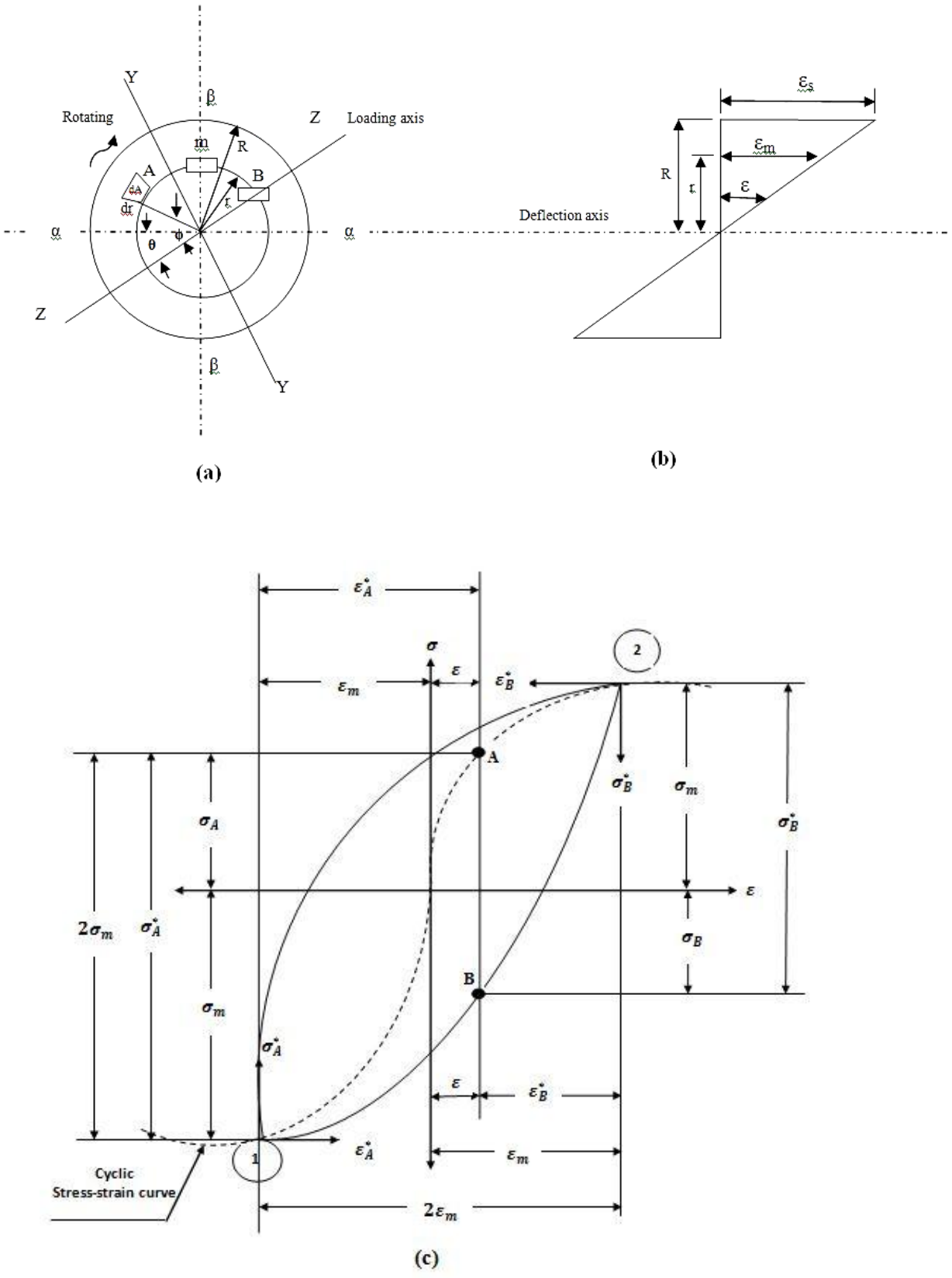

Fig. 2.16 Stress distribution in rotating bending from axial strain cyclic properties

The following relation for the shape of a hysteresis loop is obtained by applying the Masing rule:

$$\varepsilon^* = \left(\frac{\sigma^*}{2E}\right) + \left(\frac{\sigma^*}{2K'}\right)^{\frac{1}{n'}} \tag{2.9}$$

Points (1) and (2) in Fig. 2.16*c*, which lie on the cyclic stress-strain curve, are considered to be the origins of the upper and the lower branches of the settled hysteresis loop corresponding to the strain amplitude ε_m. The upper branch is described by stress σ_A^* and strain ε_A^* as follows:

$$\varepsilon_A^* = \left[\frac{\sigma_A^*}{E}\right] + 2^{1-\frac{1}{n'}}\left[\frac{\sigma_A^*}{K'}\right]^{\frac{1}{n'}} \tag{2.10}$$

The lower branch is described by stress σ_B^* and strain ε_B^* as follows:

$$\varepsilon_B^* = \left[\frac{\sigma_B^*}{E}\right] + 2^{1-\frac{1}{n'}}\left[\frac{\sigma_B^*}{K'}\right]^{\frac{1}{n'}} \tag{2.11}$$

Stresses σ_A and σ_B can then be determined from this settled hysteresis loop with strain range $2\varepsilon_m$, as shown in Fig. 2.16*c*, and given as

$$\sigma_B = \sigma^*_B - \sigma_m \tag{2.12}$$

$$\sigma_A = \sigma^*_A - \sigma_m \tag{2.13}$$

Therefore stresses σ^*_A, σ^*_B, and ε_m, should be determined first prior to calculating σ_A and σ_B. Points (1) and (2) in Fig. 2.16*c* lie on the cyclic stress-strain curve described by Eq. (2.8). Hence, ε_m is given as

$$\varepsilon_m = \left(\frac{\sigma_m}{E}\right) + \left(\frac{\sigma_m}{K'}\right)^{\frac{1}{n'}} \tag{2.14}$$

Considering Eq. (2.14) and making the necessary manipulations yields

$$\sigma^{\frac{1}{n'}}{}_m + (K')^{\frac{1}{n'}}.\frac{\sigma_m}{E} - (K')^{\frac{1}{n'}}.\frac{r}{R}\varepsilon_s = 0 \tag{2.15}$$

This is a non-linear equation in ε_m, which can be solved for all generic radii $0 \le r \le R$ by the Newton- Raphson method. Referring again to Fig. 2.16*a*, points A and B are defined by the radius r and the angle θ. The angle θ is measured clockwise, in the direction of rotation. Figure 2.17 shows that points A and B are at the strain level ε. Strain relationships can be determined as follows:

$$\varepsilon = \varepsilon_m sin\theta \tag{2.16}$$

$$\varepsilon_A^{\ *} = \varepsilon + \varepsilon_m = \varepsilon_m(1+\sin\theta) \tag{2.17}$$

$$\varepsilon^*{}_B = \varepsilon - \varepsilon_m = \varepsilon_m(1-\sin\theta) \tag{2.18}$$

Considering Eq. (2.7), the final expressions for $\sigma^*{}_A$ and $\sigma^*{}_B$ are obtained as

$$\varepsilon^*{}_A = (1+\sin\theta)\left(\frac{r}{R}\right)\varepsilon_s \tag{2.19}$$

$$\varepsilon^*{}_B = (1+\sin\theta)\left(\frac{r}{R}\right)\varepsilon_s \tag{2.20}$$

Substituting Eq. (2.19) into Eq. (2.10) yields

$$(\sigma^*{}_A)^{\frac{1}{n'}} + (2^{1-n'}K')^{\frac{1}{n'}}\left(\frac{\sigma^*{}_A}{E}\right) - (2^{1-n'}K')^{\frac{1}{n'}}(1+\sin\theta)\left(\frac{\mathrm{r}}{R}\right)\varepsilon_s = 0 \tag{2.21}$$

Similarly, substituting Eq. (2.20) into Eq. (2.11) yields

$$\left(\sigma^*{}_B\right)^{\frac{1}{n'}} + (2^{1-n'}K')^{\frac{1}{n'}}\left(\frac{\sigma^*{}_B}{E}\right) - (2^{1-n'}K')^{\frac{1}{n'}}(1-\sin\theta)\left(\frac{r}{R}\right)\varepsilon_s = 0 \tag{2.22}$$

Solving Eqs. (2.21) and (2.22) by Newton-Raphson method, $\sigma^*{}_A$ and $\sigma^*{}_B$ can be determined at any point defined by *r* and θ, under applied surface strain ε_s.

Once $\sigma^*{}_A$, $\sigma^*{}_B$ and σ_m are determined, the stresses σ_A and σ_B can be determined from Eqs. (2.12) and (2.13). The complete stress distribution can now be described with respect to the deflection axis $\alpha\alpha$, whose direction has not yet been determined with respect to the loading axis ZZ. Hence the hysteresis angle ϕ between these two axes must first be determined prior to establishing the final stress distribution with respect to the loading axis. A typical element of area *dA* located at angle θ and radius *r,* is considered as shown as in Fig. 2.16*a*, where θ is measured clockwise from the negative direction of the deflection axis $\alpha\alpha$. The bending moments about the axes $\alpha\alpha$, ZZ and *YY* are given as

$$M_{\alpha\alpha} = \int_A \sigma dA r\sin\theta; M_{\beta\beta} = \int_A \sigma dA r\cos\theta \tag{2.23}$$

$$M_{zz} = \int_A \sigma dA r\sin(\theta+\phi); M_{yy} = \int_A \sigma dA r\cos(\theta+\phi) \tag{2.24}$$

$$M_{zz} = \cos\phi\int_A \sigma dA r\sin\theta + \sin\phi\int_A \sigma dA r\cos\theta \tag{2.25}$$

At a specified cyclic loading condition, and at a fixed value of ϕ, the bending moments about the axes ZZ and YY can be rewritten as follows:

$$M_{yy} = \cos\phi\int_A \sigma dA r\cos\theta + \sin\phi\int_A \sigma dA r\sin\theta \tag{2.26}$$

Substituting Eqs. (2.23) and (2.24) in Eqs. (2.25) and (2.26) yields

$$M_{zz} = M_{\alpha\alpha}\cos\phi + M_{\beta\beta}\sin\phi \tag{2.27}$$

$$M_{yy} = M_{\beta\beta}\cos\phi + M_{\alpha\alpha}\sin\phi \tag{2.28}$$

Note that the bending moment about the YY axis vanishes; hence

$$\phi = \tan^{-1}\left(\frac{M_{\beta\beta}}{M_{\alpha\alpha}}\right) \tag{2.29}$$

Values of $M\alpha\alpha$ and $M_{\beta\beta}$ are obtained from Eqs. (2.23) and (2.24) as

$$M_{\alpha\alpha} = \int_0^{\frac{\pi}{2}}\int_0^R \sigma_A r^2\cos\theta dr d\theta + \int_{\frac{\pi}{2}}^{\pi}\int_0^R \sigma_B r^2\cos\theta dr d\theta + \int_{\pi}^{2\pi}\int_0^R \sigma_B r^2\cos\theta dr d\theta + \int_{2\pi/0}^{\pi}\int_0^R \sigma_A r^2\cos\theta dr d\theta \tag{2.30}$$

$$M_{\alpha\alpha} = \int_0^{\frac{\pi}{2}}\int_0^R \sigma_A r^2\sin\theta dr d\theta + \int_{\frac{\pi}{2}}^{\pi}\int_0^R \sigma_B r^2\sin\theta dr d\theta + \int_{\pi}^{\frac{3\pi}{2}}\int_0^R \sigma_B r^2\sin\theta dr d\theta + \int_{3\pi/2}^{\pi}\int_0^R \sigma_A r^2\sin\theta dr d\theta \tag{2.31}$$

Referring to the stress-strain relations as shown in Fig. 2.16*c* and making the necessary manipulations, Eqs. (2.30) and (2.31) can be rewritten as follows:

$$M_{\alpha\alpha} = 2\left(\int_0^{\frac{\pi}{2}}\int_0^R \sigma_A r^2\cos\theta dr d\theta + \int_0^{\frac{\pi}{2}}\int_0^R \sigma_B r^2\sin\theta dr d\theta\right) \tag{2.32}$$

$$M_{\beta\beta} = 2\left(\int_0^{\frac{\pi}{2}}\int_0^R \sigma_A r^2\cos\theta dr d\theta - \int_0^{\frac{\pi}{2}}\int_0^R \sigma_B r^2\cos\theta dr d\theta\right) \tag{2.33}$$

The above double integrals are determined numerically, by Simpson's rule for double integration, for any given values of the three material constants *K'*, *n'* and *E*, the surface strain ε_s and the radius *R*. Once $M_{\alpha\alpha}$, and $M_{\beta\beta}$ have been obtained, the hysteresis angle ϕ can he determined from Eq. (2.29). Then the bending stress can be obtained from the relation given by

$$\sigma_b = \frac{4M_{zz}}{\pi R^3} \tag{2.34}$$

The bending moment M_{zz}, required for the prescribed surface strain ε_s, is obtained from Eq. (2.27), with the corresponding elastically calculated surface bending stress, σ_b is obtained from Eq. (2.34).

So far, the procedure adopted to predict the rotating bending fatigue data for a material from the knowledge of its cyclic stress-strain response (*n'* and *K'*) and modulus of elasticity *E* has been illustrated. It is intended here to carry out the reverse procedure: i.e. to determine the cyclic stress-strain response for a material from the knowledge of its rotating bending fatigue data, namely: (a) the applied nominal bending stress, σ_b (thus bending moment M_{zz}); (b) the corresponding induced surface strain amplitude, ε_s, and (c) the corresponding experimental hysteresis angle $\phi_{\exp}$. Making use of Eqs. (2.12), (2.13), (2.15), (2.21) and (2.22), which provide the values of stress at any given point (r,θ) in the tested section, the equilibrium Eqs. (2.32) and (2.33) can be rewritten as follows:

$$M_{\alpha\alpha} = M_{zz}\cos\phi_{\exp} = \int_0^{\pi/2}\int_0^R F_1(n', K'E, \varepsilon_s, R, r, \theta)drd\theta + \int_0^{\pi/2}\int_0^R F_2(n', K', E, \varepsilon_s.R, r, \theta)drd\theta \quad (2.35)$$

$$M_{\beta\beta} = M_{zz}\cos\phi_{\exp} = \int_0^{\frac{\pi}{2}}\int_0^R F_3(n', K, E, \varepsilon_s, R, r, \theta)drd\theta + \int_0^{\pi/2}\int_0^R F_4(n'K', E, \varepsilon_s R, r, \theta)drd\theta \quad (2.36)$$

Equations (2.35) and (2.36) represent two non-linear equations involving double integration where all quantifies are known except *n'* and *K'*. Substituting the expression for M_{zz} from Eq. (2.25) into Eq. (2.35), following expression is obtained

$$M_{\alpha\alpha} = \int_0^{\frac{\pi}{2}}\int_0^R \left[\sigma_A\{Cos\phi Sin\theta + Sin\phi Cos\theta\}2Cos\phi_{exp}\right]r^2 drd\theta$$

$$+ \int_0^{\frac{\pi}{2}}\int_0^R \left[\sigma_B\{Cos\phi Sin\theta - Sin\phi Cos\theta\}2Cos\phi_{exp}\right]r^2 drd\theta \quad (2.37)$$

Considering F= $M_{\alpha\alpha}$ and

$$F_1 = 2r^2 Cos\phi_{exp}\{Cos\phi Sin\theta + Sin\phi Cos\theta\} \quad (2.38)$$

$$F_2 = 2r^2 Cos\phi_{exp}\{Cos\phi Sin\theta - Sin\phi Cos\theta\}\sigma_B \quad (2.39)$$

Equation (2.37) is rewritten as

$$F = \int_0^{\frac{\pi}{2}} \int_0^R F_1 dr d\theta + \int_0^{\frac{\pi}{2}} \int_0^R F_2 dr d\theta \quad (2.40)$$

Again, substituting the expression for M_{zz} from Eq. (2.25) into Eq. (2.36), following expression is obtained

$$M_{\beta\beta} = \int_0^{\frac{\pi}{2}} \int_0^R \left[\sigma_A \{Sin\phi Sin\theta + Cos\phi Cos\theta\} 2Sin\phi_{exp}\right] r^2 dr d\theta + \int_0^{\frac{\pi}{2}} \int_0^R \left[\sigma_B \{Sin\phi Sin\theta - Cos\phi Cos\theta\} 2Sin\phi_{exp}\right] r^2 dr d\theta \quad (2.41)$$

Considering G= $M_{\beta\beta}$ and

$$G_1 = 2r^2 Sin\phi_{exp}\{Sin\phi Sin\theta + Cos\phi Cos\theta\}\sigma_A \quad (2.42)$$

$$G_2 = 2r^2 Sin\phi_{exp}\{Sin\phi Sin\theta - Cos\phi Cos\theta\}\sigma_B \quad (2.43)$$

Equation (2.41) can be rewritten as

$$G = \int_0^{\frac{\pi}{2}} \int_0^R G_1 dr d\theta + \int_0^{\frac{\pi}{2}} \int_0^R G_2 dr d\theta \quad (2.44)$$

Equations (2.40) and (2.44) can be recast as follows:

$$F(n', K') = 0 \quad (2.45)$$

$$G(n', K') = 0 \tag{2.46}$$

Equations (2.45) and (2.46) can he solved by a series expansion technique. Suppose that (n_o, K_o) is an approximate solution, and let *dn* and *dK* be corrections to be determined. Therefore, Eqs. (2.45) and (2.46) can be written as

$$F\left(n_0^{'} + dn^{'}, K_0^{'} + dK^{'}\right) = 0 \tag{2.47}$$

$$G\left(n_0^{'} + dn^{'}, K_0^{'} + dK^{'}\right) = 0 \tag{2.48}$$

Expanding Eqs. (2.47) and (2.48) by Taylor series, and truncating after the first-order terms, yields

$$F\left(n_0^{'}, K_0^{'}\right) + dn^{'}\left(\frac{\partial F}{\partial n^{'}}\right)_0 + dK^{'}\left(\frac{\partial F}{\partial n^{'}}\right)_0 = 0 \tag{2.49}$$

$$G\left(n_0^{'}, K_0^{'}\right) + dn^{'}\left(\frac{\partial G}{\partial n^{'}}\right)_0 + dK^{'}\left(\frac{\partial G}{\partial n^{'}}\right)_0 = 0 \tag{2.50}$$

Equations (2.49) and (2.50) can be written in matrix form as

AX=Y (2.51)

Where

$$A = \begin{bmatrix} \left(\frac{\partial F}{\partial n}\right)_0 & \left(\frac{\partial F}{\partial K}\right)_0 \\ \left(\frac{\partial G}{\partial n}\right)_0 & \left(\frac{\partial G}{\partial K}\right)_0 \end{bmatrix}$$

$$X = \begin{bmatrix} dn^{'} \\ dk^{'} \end{bmatrix}$$

$$Y = \begin{bmatrix} -F(n_0, K_0) \\ -G(n_0, K_0) \end{bmatrix}$$

The differentiation terms appearing in Eqs. (2.49) and (2.50) are obtained as

$$\frac{\partial F}{\partial n'} = \int_0^{\frac{\pi}{2}} \int_0^R 2r^2 Cos\phi_{exp}\{Cos\phi Sin\theta + Sin\phi Cos\theta\}\left\{\frac{\partial \sigma_A^*}{\partial n'} - \frac{\partial \sigma_m}{\partial n'}\right\} dr d\theta$$

$$+ \int_0^{\frac{\pi}{2}} \int_0^R 2r^2 Cos\phi_{exp}\{Cos\phi Sin\theta - Sin\phi Cos\theta\}\left\{\frac{\partial \sigma_B^*}{\partial n'} - \frac{\partial \sigma_m}{\partial n'}\right\} dr d\theta \qquad (2.52)$$

$$\frac{\partial F}{\partial k'} = \int_0^{\frac{\pi}{2}} \int_0^R 2r^2 Cos\phi_{exp}\{Cos\phi Sin\theta + Sin\phi Cos\theta\}\left\{\frac{\partial \sigma_A^*}{\partial k'} - \frac{\partial \sigma_m}{\partial k'}\right\} dr d\theta$$

$$+ \int_0^{\frac{\pi}{2}} \int_0^R 2r^2 Cos\phi_{exp}\{Cos\phi Sin\theta - Sin\phi Cos\theta\}\left\{\frac{\partial \sigma_B^*}{\partial k'} - \frac{\partial \sigma_m}{\partial k'}\right\} dr d\theta \qquad (2.53)$$

$$\left(\frac{\partial F}{\partial n'}\right)_0 = \left(\frac{\partial F}{\partial n'}\right)_{(n_0', k_0')} \qquad (2.54)$$

$$\left(\frac{\partial F}{\partial k'}\right)_0 = \left(\frac{\partial F}{\partial k'}\right)_{(n_0', k_0')} \qquad (2.55)$$

$$\frac{\partial G}{\partial n'} = \int_0^{\frac{\pi}{2}} \int_0^R 2r^2 Sin\phi_{exp}\{Sin\phi Sin\theta + Cos\phi Cos\theta\}\left\{\frac{\partial \sigma_A^*}{\partial n'} - \frac{\partial \sigma_m}{\partial n'}\right\} dr d\theta$$

$$+ \int_0^{\frac{\pi}{2}} \int_0^R 2r^2 Sin\phi_{exp}\{Sin\phi Sin\theta - Cos\phi Cos\theta\}\left\{\frac{\partial \sigma_B^*}{\partial n'} - \frac{\partial \sigma_m}{\partial n'}\right\} dr d\theta \qquad (2.56)$$

$$\frac{\partial G}{\partial k'} = \int_0^{\frac{\pi}{2}} \int_0^R 2r^2 Sin\phi_{exp}\{Sin\phi Sin\theta + Cos\phi Cos\theta\}\left\{\frac{\partial \sigma_A^*}{\partial k'} - \frac{\partial \sigma_m}{\partial k'}\right\} dr d\theta$$

$$+ \int_0^{\frac{\pi}{2}} \int_0^R 2r^2 Sin\phi_{exp}\{Sin\phi Sin\theta - Cos\phi Cos\theta\}\left\{\frac{\partial \sigma_B^*}{\partial k'} - \frac{\partial \sigma_m}{\partial k'}\right\} dr d\theta \qquad (2.57)$$

$$\left(\frac{\partial G}{\partial n'}\right)_0 = \left(\frac{\partial G}{\partial n'}\right)_{(n_0',k_0')} \tag{2.58}$$

$$\left(\frac{\partial G}{\partial k'}\right)_0 = \left(\frac{\partial G}{\partial k'}\right)_{(n_0',k_0')} \tag{2.59}$$

$$\left(\frac{\partial \sigma_A^*}{\partial n'}\right)$$

$$= \frac{\left[\left(2^{\frac{1}{n'}-1}\right)(ln2)(k')^{\frac{1}{n'}} + \left(2^{\frac{1}{n'}-1}\right)(k')^{\frac{1}{n'}}(lnk')\right]\left\{(1+Sin\theta)\frac{r}{R}\varepsilon_s\right\} - \left[\left(2^{\frac{1}{n'}-1}\right)(k')^{\frac{1}{n'}}(lnk')\left(\frac{\sigma_A^*}{E}\right) + \left(2^{\frac{1}{n'}-1}\right)(k')^{\frac{1}{n'}}\left(\frac{1}{E}\right)\right]}{\left[\frac{1}{n'}(\sigma_A^*)^{\frac{1}{n'}-1} + (2^{1-n'}k')^{\frac{1}{n'}}\frac{1}{E}\right]} \tag{2.60}$$

$$\left(\frac{\partial \sigma_B^*}{\partial n'}\right)$$

$$= \frac{\left[\left(2^{\frac{1}{n'}-1}\right)(ln2)(k')^{\frac{1}{n'}} + \left(2^{\frac{1}{n'}-1}\right)(k')^{\frac{1}{n'}}(lnk')\right]\left\{(1-Sin\theta)\frac{r}{R}\varepsilon_s\right\} - \left[\left(2^{\frac{1}{n'}-1}\right)(k')^{\frac{1}{n'}}(lnk')\left(\frac{\sigma_B^*}{E}\right) + \left(2^{\frac{1}{n'}-1}\right)(k')^{\frac{1}{n'}}\left(\frac{1}{E}\right)\right]}{\left[\frac{1}{n'}(\sigma_B^*)^{\frac{1}{n'}-1} + (2^{1-n'}k')^{\frac{1}{n'}}\frac{1}{E}\right]} \tag{2.61}$$

$$\frac{\partial \sigma_m}{\partial n'}\left[\frac{1}{n'}(\sigma_m)^{\frac{1}{n'}-1} + \frac{(k')^{\frac{1}{n'}}}{E}\right] = 0 \tag{2.62}$$

$$\left(\frac{\partial \sigma_A^*}{\partial k'}\right) = \frac{\left(2^{\frac{1}{n'}-1}\right)(k')^{\frac{1}{n'}-1}\left\{(1+Sin\theta)\frac{r}{R}\varepsilon_s - \frac{\sigma_A^*}{E}\right\}}{\left(\frac{1}{n'}(\sigma_A^*)^{\frac{1}{n'}-1}\right) + \left(2^{\frac{1}{n'}-1}\right)(k')^{\frac{1}{n'}}\left(\frac{1}{E}\right)} \tag{2.63}$$

$$\left(\frac{\partial \sigma_B^*}{\partial k'}\right) = \frac{\left(2^{\frac{1}{n'}-1}\right)(k')^{\frac{1}{n'}-1}\left\{(1-Sin\theta)\frac{r}{R}\varepsilon_s - \frac{\sigma_B^*}{E}\right\}}{\left(\frac{1}{n'}(\sigma_B^*)^{\frac{1}{n'}-1}\right) + \left(2^{\frac{1}{n'}-1}\right)(k')^{\frac{1}{n'}}\left(\frac{1}{E}\right)} \tag{2.64}$$

$$\frac{\partial \sigma_m}{\partial k'} = \frac{\left[\frac{1}{n'}(k')^{\frac{1}{n'}-1}\left\{\frac{r}{R}\varepsilon_s - \frac{\sigma_m}{E}\right\}\right]}{\left[\frac{1}{n'}(\sigma_m)^{\frac{1}{n'}-1} + \frac{(k')^{\frac{1}{n'}}}{E}\right]} \tag{2.65}$$

$$\frac{\partial \sigma_m}{\partial n'} = \frac{\left[(k')^{\frac{1}{n'}} ln k' \left\{ \frac{r}{R} \varepsilon_s - \frac{\sigma_m}{E} \right\} \right]}{\left[\frac{1}{n'} (\sigma_m)^{\frac{1}{n'}-1} + \frac{(k')^{\frac{1}{n'}}}{E} \right]} \tag{2.66}$$

The two linear equations given by Eqs. (2.49) and (2.50) in dn' and dK' can he solved to give the next approximation. The final values of *n'* and *K'* can be determined by carrying out an iteration technique until the values of dn' and dK' become negligible. Input data consists of applied nominal bending stress σ_b, corresponding surface strain amplitude ε_s , corresponding experimental hysteresis angle $\phi_{\exp}$ and the modulus of elasticity *E*.

An initial guess n_0' *and* K_0' is made for the two unknowns n' and K'. After carrying out the iteration procedure, the final values of n' and K', and hence the corresponding true stress σ and surface plastic strain amplitude $\varepsilon^p{}_s$ are determined for the test specimen.

2.5 Empirical Analysis

2.5.1 Monotonic Loading

When a metal is monotonically loaded, elastic and plastic strains can occur, and it is possible to determine the tensile monotonic behavior of a metallic material using the Ramberg-Osgood relation given by

$$\varepsilon = \left(\frac{\sigma}{E}\right) + \left(\frac{\sigma}{K}\right)^{\frac{1}{n}} \tag{2.67}$$

The parameters n and k appearing in Eq. (2.8) can be estimated from empirical relations given below [44]:

$$n = \frac{log\left(\frac{\sigma_f^3 \sigma_{ult}^2}{\sigma_y^5}\right)}{3log(500\varepsilon_f)} \quad , \quad k = \sigma_f \ \varepsilon_f^{-n} \qquad (2.68)$$

$$6.38n = \frac{log\left(\frac{\sigma_f^2}{\sigma_y \sigma_{ult}}\right)}{2log(500\varepsilon_f)} \quad , \quad k = \frac{\sigma_f \sigma_y}{\sigma_{ult}} \ \varepsilon_f^{-n} \qquad (2.69)$$

$$n = \frac{log\left(\frac{\sigma_f}{\sigma_y}\right)}{log(500\varepsilon_f)} \quad , \quad k = 500^n \sigma_y \qquad (2.70)$$

Where *n* is strain hardening exponent, *k* is strength coefficient, σ_{ys} is the yield stress, σ_{ult} is the ultimate stress, σ_f is fracture stress and ε_f fracture strain.

2.5.2 Cyclic Loading

For cyclically loaded metallic material under a constant strain internal , the hysteresis loop tends to get stabilized even after cyclic softening or hardening resulting in a static value of Δσ for a given Δε . The cyclic stress-strain curve is described by Ramberg-Osgood relation and is given by Eq. (2.8).

Fatigue failure of metallic materials occurs after a number of cycles during cyclic loading as a result of nucleation and growth of fatigue crack. The empirical relationship used to define total number of cycles to fatigue failure of metallic materials is given by Eq. (2.4).

2.6 Empirical life prediction for smooth specimen

2.6.1 Smith, Watson and Topper (SWT) parameter

SWT parameter is based on the assumption that the product between σ_{max} and σ_a is constant for a given number of cycles to failure, including different combination of strain amplitude and mean stress as given by [45]:

$$\sigma_{max}\,\varepsilon_a\,E = \left(\sigma_f^{'}\right)^2\left(2N_f\right)^{2b} + \sigma_f^{'}\,\varepsilon_f^{'}E\left(2N_f\right)^{b+c} \tag{2.71}$$

Chion [46] demonstrated the calculation of strain amplitude (ε_a) using a modified cyclic stress-strain curve for any loading, considering mean strain stress effect and different H^* and n^* values instead of K^* and $K^{'}$, leading to modified SWT parameter given by:

$$\sigma_{max}\left[\frac{\sigma_{max}}{E} + \left(\frac{\sigma_{max}}{\mathrm{K}*}\right)^{\frac{1}{n*}}\right]E = \left(\sigma_f^{'}\right)^2\left(2N_f\right)^{2b} + \sigma_f^{'}\,\varepsilon_f^{'}E\left(2N_f\right)^{b+c} \tag{2.72}$$

2.6.2 Morrow relationship

Morrow [47] proposes a new equation to consider the influence of the mean stress, where elastic and plastic terms were affected by mean stress given as

$$\varepsilon_a = \frac{\sigma_f^{'}}{E}\left[2N_f\left(1-\frac{\sigma_m}{\sigma_f^{'}}\right)^{\frac{1}{b}}\right]^b + \varepsilon_f^{'}[2N_f]^c \tag{2.73}$$

The equivalent number of cycles of failure (N^*) in a zero mean stress loading is given as

$$N^* = N_f\left(1-\frac{\sigma_m}{\sigma_f^{'}}\right)^{\frac{1}{b}} \tag{2.74}$$

In Eqs. (2.71) to (2.74) , fatigue strength and ductility exponents (b and c) values do not vary when the applied loading is changed. These constants are obtained using fatigue data obtained during tests with zero mean stress and strain.

2.6.3 Walker relationship

According to walker [48] N_f due to applied ε_a at any R_σ ratio, can be related and given as

$$\varepsilon_a = \frac{\sigma_{fw}^{'}}{E}\left[2N_f\left(\frac{1-R\sigma}{2}\right)^{\frac{1-v}{bw}}\right]^{bw} + \varepsilon_{fw}^{'}\left[2N_f\left(\frac{1-R\sigma}{2}\right)^{\frac{1-v}{bw}}\right]^{cw}$$

(2.75)

Where

$$R_\sigma = \frac{\sigma_{min}}{\sigma_{max}} \quad (2.76)$$

Applied strain amplitude can be related to an equivalent number of cycles to fatigue in a zero mean stress loading (N^*) as

$$N^* = N_f\left(\frac{1-R}{2}\right)^{\frac{1-v}{bw}} \quad (2.77)$$

2.6.4 Hollomon equation

Hollomon [45] quantitatively represented cyclic stress correlation as

$$\frac{\Delta\varepsilon_a}{2E} = \frac{\Delta\sigma_e}{2E} + \left(\frac{\Delta\sigma_a}{2K}\right)^{\frac{1}{n}}\left[\frac{\Delta\sigma_a}{2} - K\left(\frac{\Delta\varepsilon_p}{2}\right)^n\right] \quad (2.78)$$

Where *n* is strain hardening exponent, *K* is strength coefficient, $\frac{\Delta\varepsilon_a}{2}$ is total strain amplitude , $\frac{\Delta\sigma_e}{2E}$ is elastic strain amplitude and $\frac{\Delta\varepsilon_p}{2}$ plastic strain amplitude .

2.7 Least Square Fit

An independent variable x and a dependent variable y is considered as y depends on x. Correlation implies a linear relationship described by the equation

y = a+bx (2.79)

Where b is the slope of the line and a is the intercept i.e. where the line cuts the **y** axis. Let a data set is strongly correlated and exhibits a linear relationship, and to fit all points best principle of least squares is used so that the sum of the squares of the deviations of all the points from the line is minimized. For each point in the dataset: y-(a+bx) measures the vertical deviation (vertical distance) from the point to the line. Some points are above the line and y-(a+bx) will be positive for these points. For points below the line y-(a+bx) will be negative. So deviations are squared to make them all positive. Now this sum of all such squared terms gives the sum of the squared distances of all the points from the line. The line which minimises this sum of squared distances is the line which fits the data best and is called Least Squares Line.

2.8 Simple linear regression model

2.8.1 Model I

The word simple here refers to the use of just one x to predict y. Problems in which two or more variables are used to predict y are called multiple regression. The input data are (x_1, y_1), (x_2, y_2), …, (x_n, y_n). The outputs are the values of b_1 (estimated regression slope) and b_0 (estimated regression intercept). The equation of fitted regression line is

$$y = b_0 + b_1 x \tag{2.80}$$

The steps for simple regression is given as

(1) Find all five sums $\sum_{i=1}^{ns} x_i$, $\sum_{i=1}^{ns} y_i$, $\sum_{i=1}^{ns} x_i^2$, $\sum_{i=1}^{ns} x_i\ y_i$

(2) Find all five expressions $\bar{x}$, $\bar{y}$ $S_{xx} = \sum_{i=1}^{n_s} x_i^2 - \frac{\left(\sum_{i=1}^{n_s} x_i\right)^2}{n_s}$

$$S_{yy} = \sum_{i=1}^{n_s} y_i^2 - \frac{\left(\sum_{i=1}^{n_s} y_i\right)^2}{n_s} \quad S_{xy} = \sum_{i=1}^{n_s} x_i y_i - \frac{\left(\sum_{i=1}^{n_s} x_i\right)\left(\sum_{i=1}^{n_s} y_i\right)}{n_s}$$

(3) Give the slope estimate as $b_1 = \frac{S_{xy}}{S_{xx}}$ and the intercept estimate as $b_0 = \bar{y} - b_1 \bar{x}$

(4) For later use, record $S_{yy|x} = S_{yy} - \frac{(S_{xy})^2}{S_{xx}}$

Virtually all the calculations for simple regression are based on the five quantities found in step (2). We use $S_{yy|x}$ to get S_ε, the estimate of the noise standard deviation. The relationship is

$$S_\varepsilon = \sqrt{\frac{S_{yy|x}}{n_s - 2}} \tag{2.81}$$

The estimate for the noise standard deviation is the square root of the mean square in the residual line. The symbol s is frequently used for this, as are $S_{y|x}$ and S_ε. The R^2 statistic is often used and is given by

$$R^2 = \frac{SS_{regr}}{SS_{resid}} \tag{2.82}$$

The standard deviation of y is given as $S_y = \sqrt{\frac{SS_{tot}}{n_s - 1}}$ (2.83)

It is sometimes interesting to compare S_ε (the estimate for the noise standard deviation) to S_Y (the standard deviation of Y). It can be shown that the ratio of these is

$$\frac{S_\varepsilon}{S_y} = \sqrt{\frac{n_s - 1}{n_s - 1 - K_R}\,(1 - R^2)} \tag{2.84}$$

The adjusted R^2 is given as

$$R^2_{adj} = 1 - \left(\frac{S_\varepsilon}{S_y}\right)^2 = 1 - \frac{n_s - 1}{n_s - 1 - K_R}\,(1 - R^2) \tag{2.85}$$

The Eqs. (2.84) and (2.85) are for K predictors and for simple regression K is used unity.

2.8.2 Model II

Let there are observations on *n* subjects consisting of a dependent or response variable *Y* and an explanatory variable *X*. Both *direction* and the *strength* of the relationship between *Y* and *X* is supposed to be measured. Two related measures are known as the *covariance* and the *correlation coefficient.* On the scatter plot of *Y* versus *X*, a vertical line at $\bar{x}$ and a horizontal line at $\bar{y}$ divide the plot into four quadrants. The quantities $\bar{y}$ and $\bar{x}$ are given as

$$\bar{y} = \frac{\sum_{i=1}^{n_s} y_i}{n_s} \tag{2.86}$$

$$\bar{x} = \frac{\sum_{i=1}^{n_s} x_i}{n_s} \tag{2.87}$$

$\bar{y}$ and $\bar{x}$ are called the sample mean of *Y* and X, respectively. For each point ***i*** in the graph, following quantities are computed $y_i - \bar{y}$, the deviation of each observation y_i from the mean of the response variable. $x_i - \bar{x}$, the deviation of each observation x_i from the mean of the predictor variable and $(y_i - \bar{y})(x_i - \bar{x})$, product of above to deviations.

It is clear that the quantity $(y_i - \bar{y})$ is positive for every point in the first and second quadrants, and is negative for every point in the third and fourth quadrants. Similarly, the quantity $(x_i - \bar{x})$ is positive for every point in the first and fourth quadrants, and is negative for every point in the second and third quadrants. If the linear relationship between Y and X is positive (as X increases Y also increases), then there are more points in the first and third quadrants than in the second and fourth quadrants. Conversely, if the relationship between Y and X is negative (as *X* increases *Y* decreases), then there are more points in the second and fourth quadrants than in the first and third quadrants. The covariance between y and x is defined as

$$Cov(Y,X)=\frac{\sum_{i=1}^{n}(y_1-\bar{y})(x_1-\bar{x})}{ns-1} \quad (2.88)$$

This quantity indicates the direction of the linear relationship between Y and X. If Cov (Y, *X)* > 0, then there is a positive relationship between *Y* and X, but if Cov (Y,X) < 0, then the relationship is negative. Unfortunately, Cov (Y,X) does not tell much about the strength of such a relationship because it is affected by changes in the units of measurement. To avoid this disadvantage of the covariance, data is *standardized* before computing the covariance. To standardize the Y data, first subtract the mean from each observation then divide by the standard deviation, that is, compute

$$z_i=\frac{y_i-\bar{y}}{s_y} \quad (2.89)$$

Where s_y is the sample standard deviation of y and is given by

$$s_y=\sqrt{\frac{\sum_{i-1}^{ns}(y_i-\bar{y})^2}{ns-1}} \quad (2.90)$$

X is also standardized in a similar way by subtracting the mean $\bar{x}$ from each observation x_i then divide by the standard deviation s_x. The covariance between the standardized X and Y data is known as the *correlation coefficient* between Y and X and is given by

$$Cor(Y,X)=\frac{1}{ns-1}\sum_{i-1}^{ns}\left(\frac{y_i-\bar{y}}{s_y}\right)\left(\frac{x_i-\bar{x}}{s_x}\right) \quad (2.91)$$

Equivalent formula for the correlation coefficient is given by

$$Cor(Y,X)=\frac{Cov(Y,X)}{s_y s_x}=\frac{\sum(y_i-\bar{y})(x_i-\bar{x})}{\sqrt{\sum(y_i-\bar{y})^2\sum(x_i-\bar{x})^2}} \quad (2.92)$$

Thus, Cor(Y, X) can be interpreted either as the covariance between the standardized variables or the ratio of the covariance to the standard deviations of the two Variables. Correlation coefficient is symmetric, that is, Cor(Y, X) = Cor(X, Y).

Unlike Cov(Y, X), Cor(Y, X) is scale invariant, that is, it does not change if we change the units of measurements. Furthermore, Cor(Y, X) satisfies

$$-1 \leq Cor\ (Y, X) \leq 1. \tag{2.93}$$

These properties make the Cor(Y,X) a useful quantity for measuring both the direction and the strength of the relationship between Y and X . The magnitude of Cor(Y, X) measures the strength of the linear relationship between Y and X . The closer Cor(Y, X) is to 1 or -1, the stronger is the relationship between Y and X . The sign of Cor(Y, X) indicates the direction of the relationship between Y and X . That is, Cor(Y, X) > 0 implies that Y and X are positively related. Conversely, Cor(Y, X) < 0, implies that Y and X are negatively related.

However, Cor(Y, X) =0 does not necessarily mean that Y and X are not related. It only implies that they are not linearly related because the correlation coefficient measures only *linear* relationships. In other words, the Cor(Y, X) can still be zero when Y and X are nonlinearly related.

2.9 Numerical Analysis

The ANSYS program has many finite element analysis capabilities ranging from a simple, linear, static analysis to complex, non-linear, transient dynamic analysis. The process for a typical ANSYS analysis involves following general tasks :

1. Building the geometrical model.

2. Discretizing the model with appropriate elements.
3. Applying geometric boundary condition.
4. Applying loads.
5. Perform appropriate analysis.
6. Obtain solution and review results.

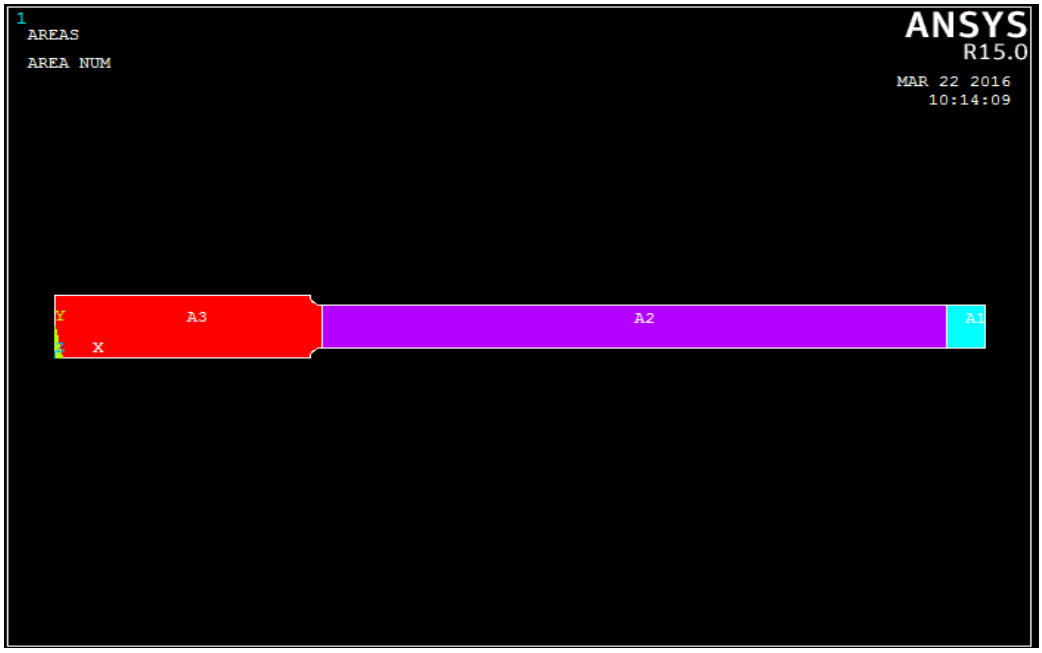

Fig. 2.17 Geometry of cantilever beam model

The current problem of rotating cantilever low cycle fatigue analysis is modeled as a two dimensional static problem by introducing centrifugal forces arising due to rotation and applying the time varying bending force at the free end [57]. The vertical section of beam is considered for analysis.

Figure 2.18 demonstrates how geometry of the current analysis is formed. Elements are created and shown in Fig. 2.19. Boundary conditions are shown in Fig.

2.20. The element used for the present analysis is PLANE182 available in Ansys software which is a two dimensional four noded structural solid element.

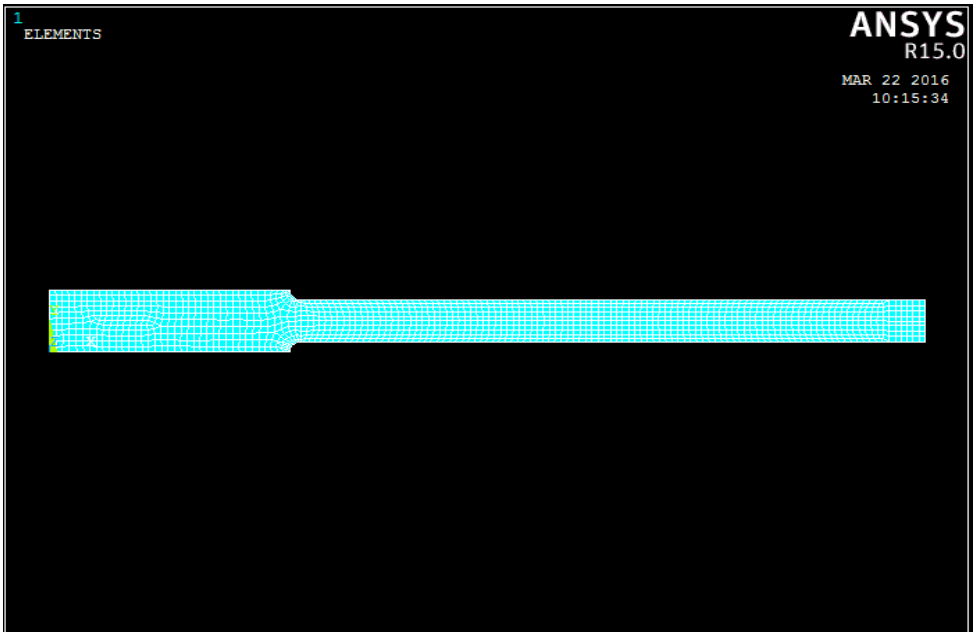

Fig. 2.18 Meshed model of cantilever beam

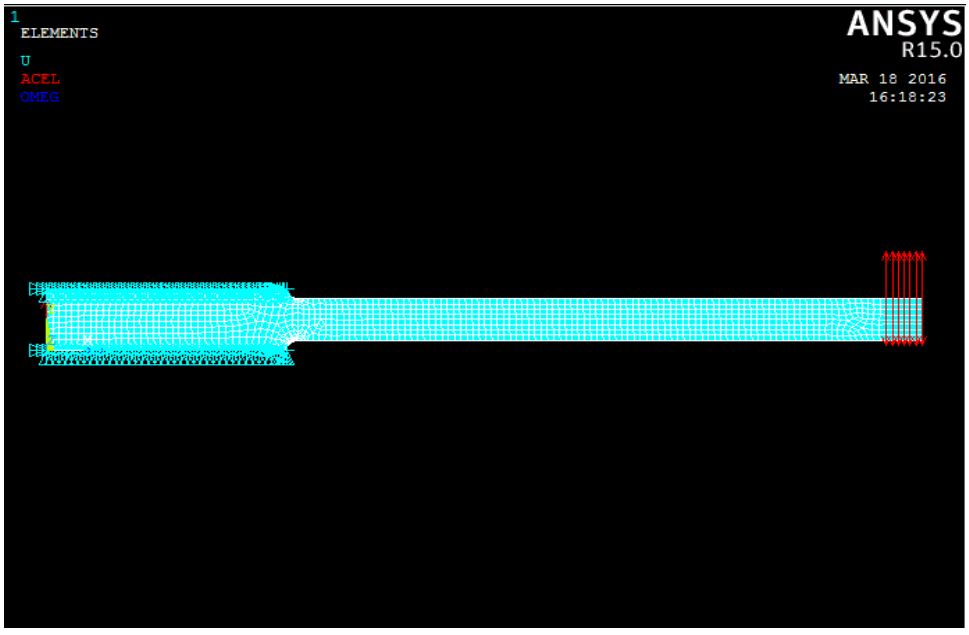

Fig. 2.19 Meshed model of cantilever beam with boundary conditions

The element is defined by four nodes having two degrees of freedom at each node viz translations in the nodal x and y directions.

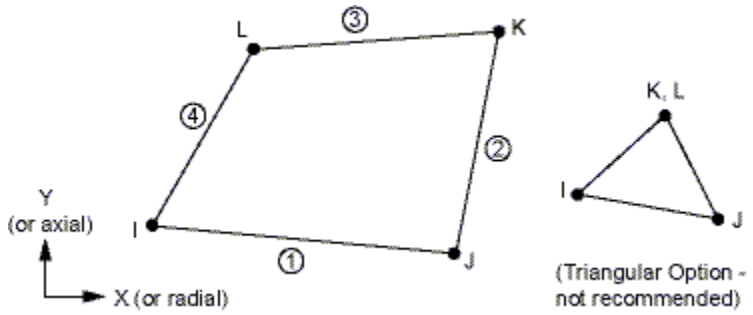

Fig. 2.20 Geometry of PLANE182 element

The geometry and node locations for this element are shown in Fig. 2.20 The element input data includes four nodes, a thickness (for the plane stress option only), and the material properties. The default element coordinate system is along global directions. The Summary of inputs for PLANE182 element are listed below

1. **Nodes:** I, J, K, L
2. **Degrees of Freedom:** UX, UY
3. **Real Constants:**

   THK - Thickness (used only if KEYOPT(3) = 3)

   HGSTF - Hourglass stiffness scaling factor (used only if KEYOPT(1) = 1); default is 1.0 (if you input 0.0, the default value is used).
4. **Material Properties**

   TB command

MP command: EX, EY, EZ, PRXY, PRYZ, PRXZ (or NUXY, NUYZ, NUXZ), ALPX, ALPY, ALPZ (or CTEX, CTEY, CTEZ *or* THSX, THSY, THSZ), DENS, GXY, GYZ, GXZ, ALPD, BETD.

5. **Loads**

   a) Pressures: face 1 (J-I), face 2 (K-J), face 3 (L-K), face 4 (I-L)

   b) Body Loads:

   Temperatures: T(I), T(J), T(K), T(L)

c) Body force densities: The element values in the global X and Y directions.

6. **KEYOPT(1):** Element technology

   a) Full integration : **0**

   b) Uniform reduced integration with hourglass control: **1**

   c) Enhanced strain formulation: **2**

   d) Simplified enhanced strain formulation: **3**

7. **KEYOPT(3):** Element behavior:

   a) Plane stress: **0**

   b) Axisymmetric: **1**

   c) Plane strain (Z strain = 0.0): **2**

   d) Plane stress with thickness input: **3**

   e) Generalized plane strain: **5**

8. **KEYOPT(6):** Element formulation:

   a) Use pure displacement formulation (default): **0**

   b) Use mixed u-P formulation (not valid with plane stress): **1**

The is the step-by-step procedure for the rotating bending low cycle fatigue analysis using the ANSYS GUI (Graphic User Interface) environment is described below

1. Main Menu

Preprocessor > Element Type > Add/Edit/Delete > Add

Structural & Solid & Quad 4 node 182

Add > DOF

Ux, Uy, Uz

2. Material Props

Material Models > Structural > Linear > Elastic > Isotropic

EX , PRXY

Material Models > Structural > nonLinear > inelastic > Rate Independent > Isotropic hardening plasticity > Mises Plasticity > Bilinear

Yield Stss, Tang Mod

Material Models > Structural > Density

DENS

3. Modeling

Create > Areas > Rectangle > By Dimensions

4. Meshing

Mesh Tool > smart size

5. Boundary Condition

Preprocessor > Loads > Define Loads > Apply > structural > Displacements > On Nodes

DOFs to be constrained = Ux, Uy, Uz

Apply as = constant value

Displacement Value = 0

Preprocessor > Loads > Define Loads > Apply > structural > Inertia > Angular Veloc > Global > Apply

OMEGX Global Cartesian X-Comp = 293.215

OMEGY Global Cartesian Y-Comp = 0

OMEGZ Global Cartesian Z-Comp = 0

Preprocessor > Loads > Define Loads > Apply > structural > Inertia > Gravity > Global > Apply

ACELX Global Cartesian X-Comp = 0

ACELY Global Cartesian Y-Comp = 981

ACELZ Global Cartesian Z-Comp = 0

6. Solution

Solution > Analysis Type > New Analysis > Transient > OK > OK

Sol'n Controls > Basic Tab

Time at end of loadstep: given

Automatic time stepping : off

Number of substep : 1

Frequency : write every Nth substep

Transient Tab

Full Transient optons > Stepped Loading & OK

Nonlinear Tab

Set convergence criteria

Default criteria to be used > replace > structural > displacement U

VALUE Reference Value of LAB

TOLER Tolerance about VALUE : 0.01

NORM Convergence norm : Infinite norm

Ok

Define Loads > Apply > Structural > Force/Moment > On Nodes

Direction of Force/Moment: FY

Force/Moment Value: OK

Load Step Opts > Write LS File

Load step file number n: *1* & OK

Analysis Type > Sol'n Controls

Basic Tab

Time at end of loadstep: OK

Define Loads > Delete > Structural > Force/Moment > On Nodes

OK

Define Loads > Apply > Structural > Force/Moment > On Nodes

Direction of Force/Moment: FY

Force/Moment Value: OK

Load Step Opts > Write LS File

Load step file number n: *2* & OK

7. Solve [Fig. 2.22 , Fig. 2.23]

From LS Files

Starting LS file number: *1*

Ending LS file number: *9*

File number increment: *1* & OK

Main Menu

General Postproc > Read Results > By Pick

Select Set 1 & Read & Close

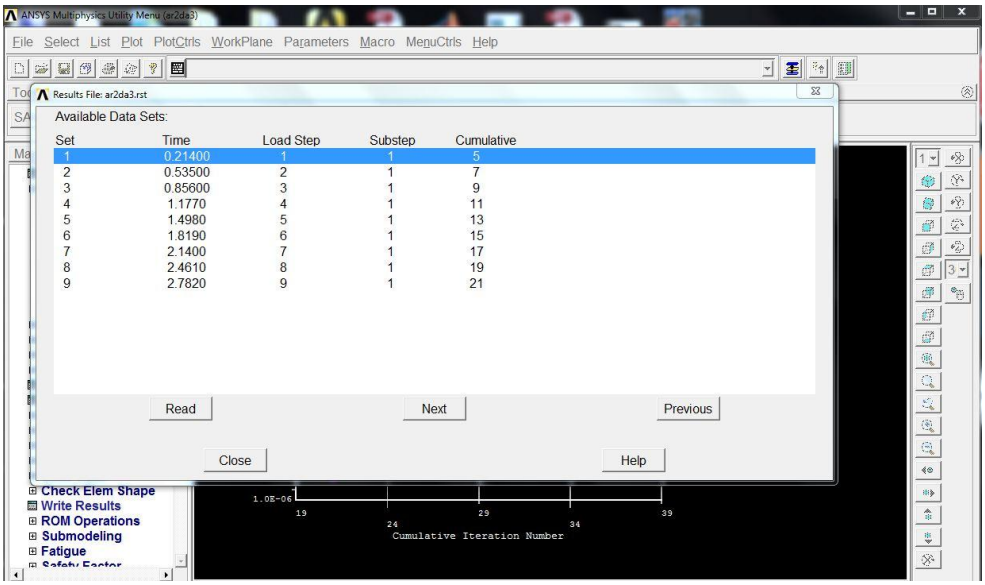

Fig. 2.21 Load step reading for set 1 from LS file

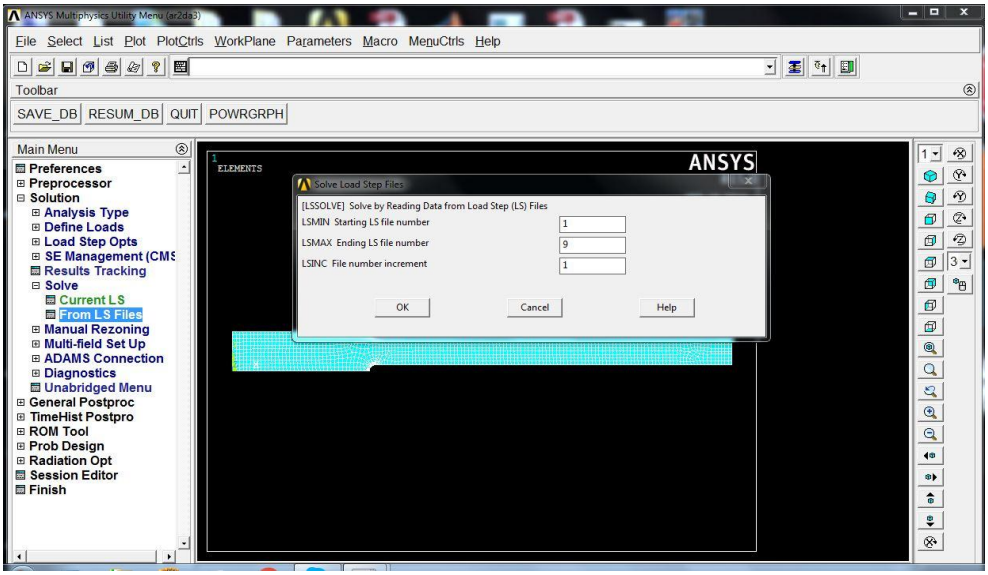

Fig. 2.22 Solution by reading data from load step

8. Steps to perform the Fatigue Analysis:

Definitions used in performing a fatigue analysis:

a) Location: a node in the model for which fatigue stresses are to be stored.

b) Event: a set of stress conditions that occur at different times during a unique stress cycle.

c) Loading: one of the stress conditions that is part of an event.

Main Menu

I. General Postproc > Fatigue > Property Table > S-N Table [Fig. 2.24].

II. Stress Locations: Stress locations are selected along the final fracture cross-section on the surface.

NLOC = 1

NODE = 3

TITLE = Top Surface

Apply

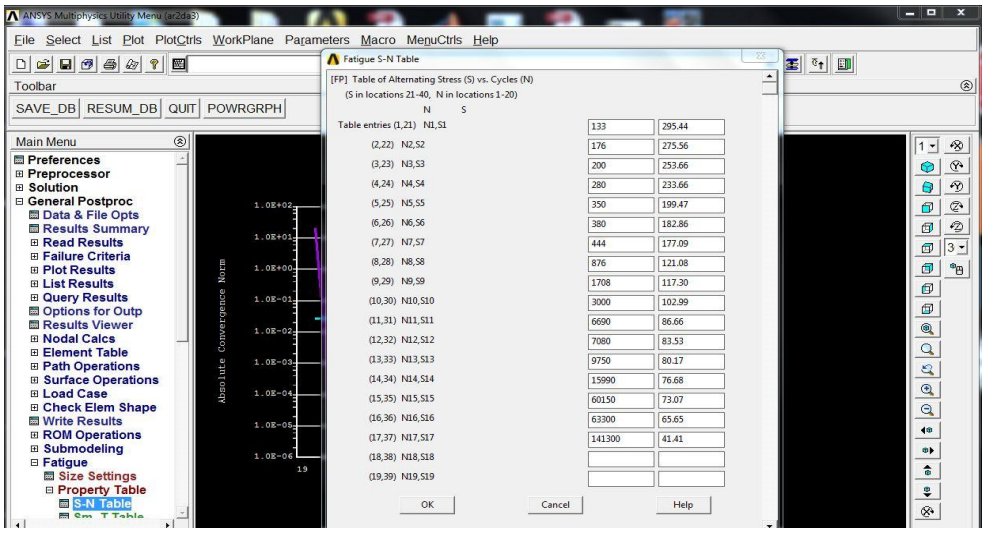

Fig. 2.23 S-N data

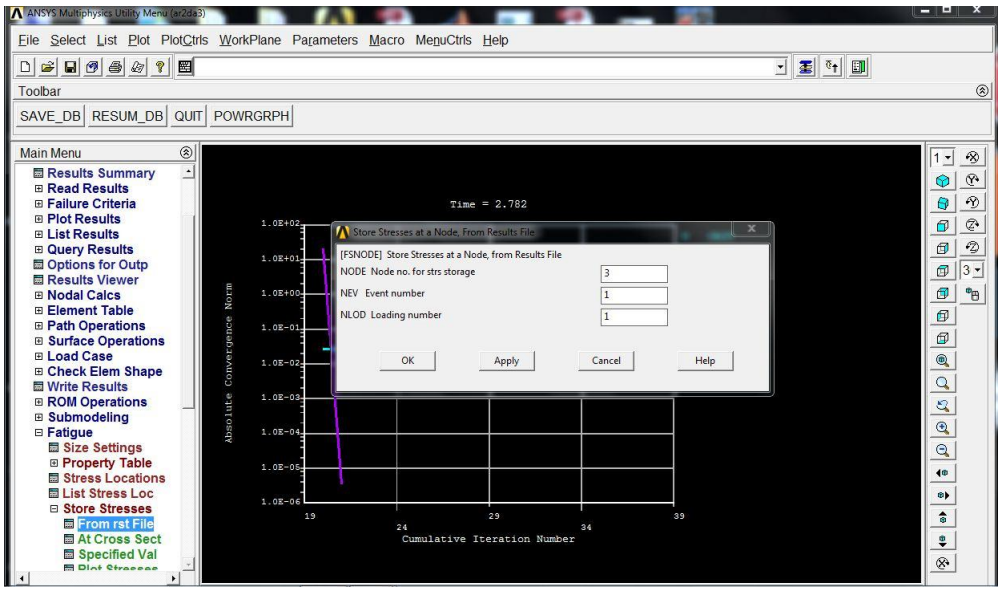

Fig. 2.24 Define node location at NLOC=1 for storing stress

III. NLOC = 2

NODE = 51

TITLE = Top Surface

Apply

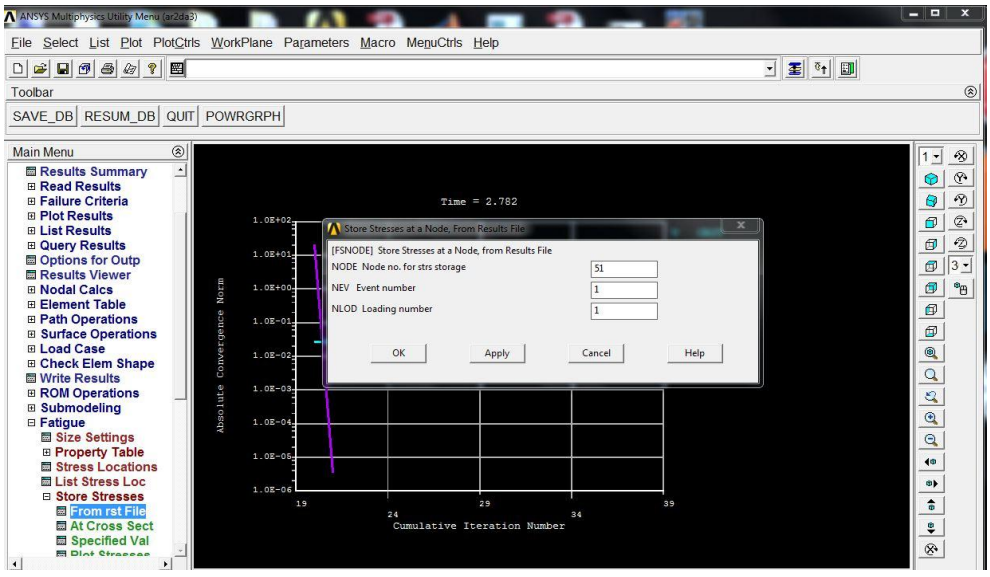

Fig. 2.25 Define node location at NLOC=2 for storing stress

IV. General Postproc > Read Results > By Pick

Select Set 2 & Read & Close Fatigue

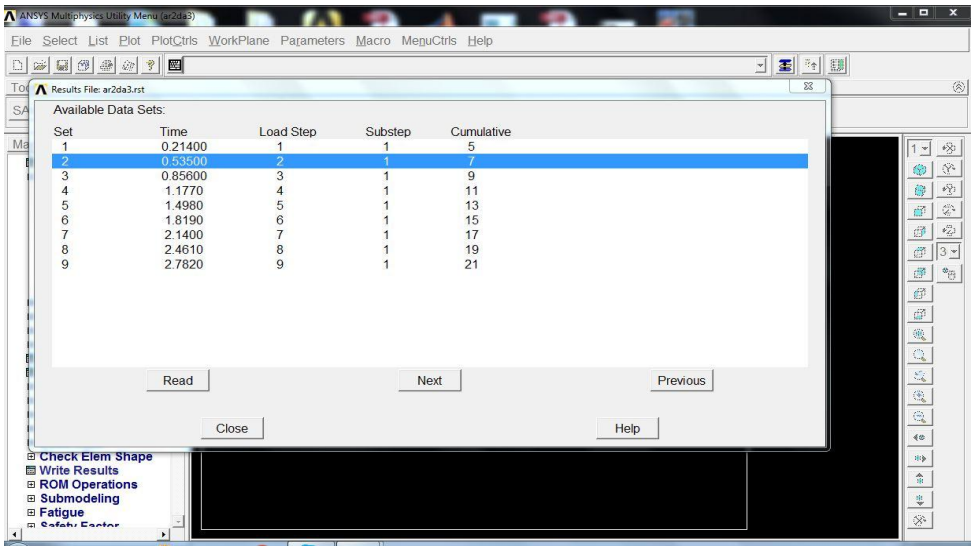

Fig. 2.26 Load step reading for set 2 from LS file

V. Store Stresses

From rst File

NODE: 3

Event: 1

Loading: 2 & Apply

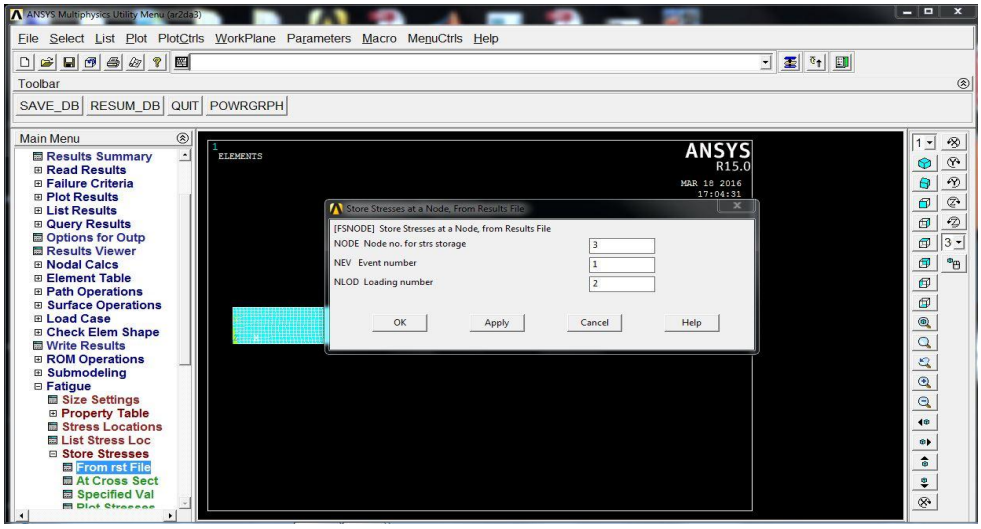

Fig. 2.27 Storing stress at NLOC=1

VI. NODE: 51

Event: 1

Loading: 2 & Apply

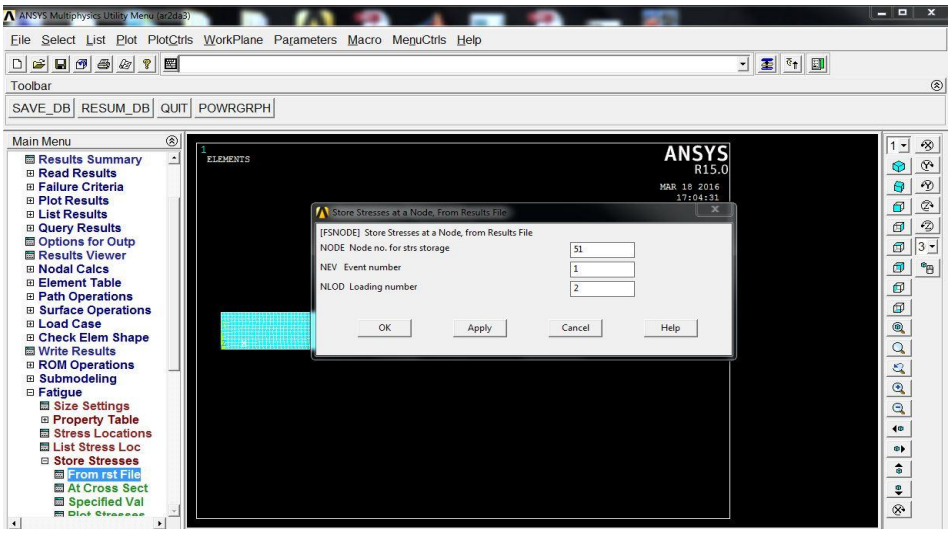

Fig. 2.28 Storing stress at NLOC=1

VII. Calculate Fatigue & OK

Assign Events

NEV = 1

CYCLE = 133

TITLE = Load 1 & Apply

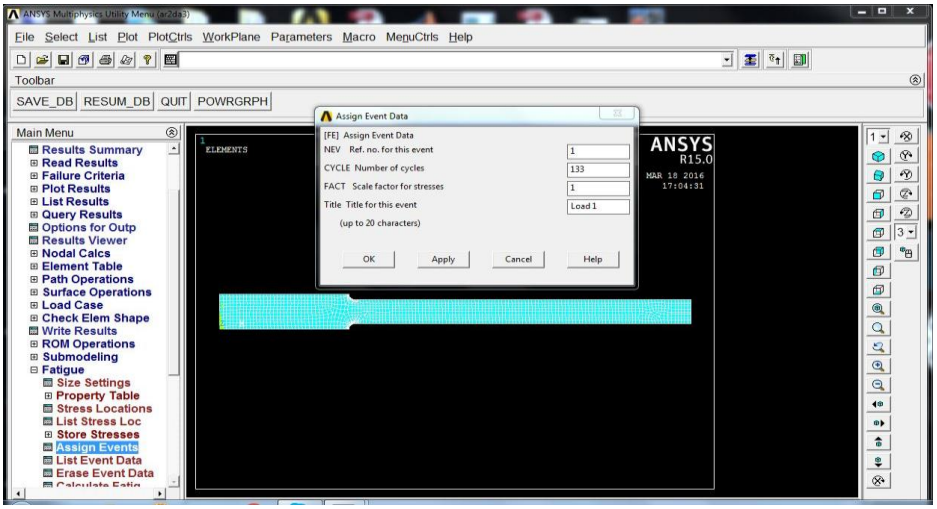

Fig. 2.29 Applying low cycle fatigue condition

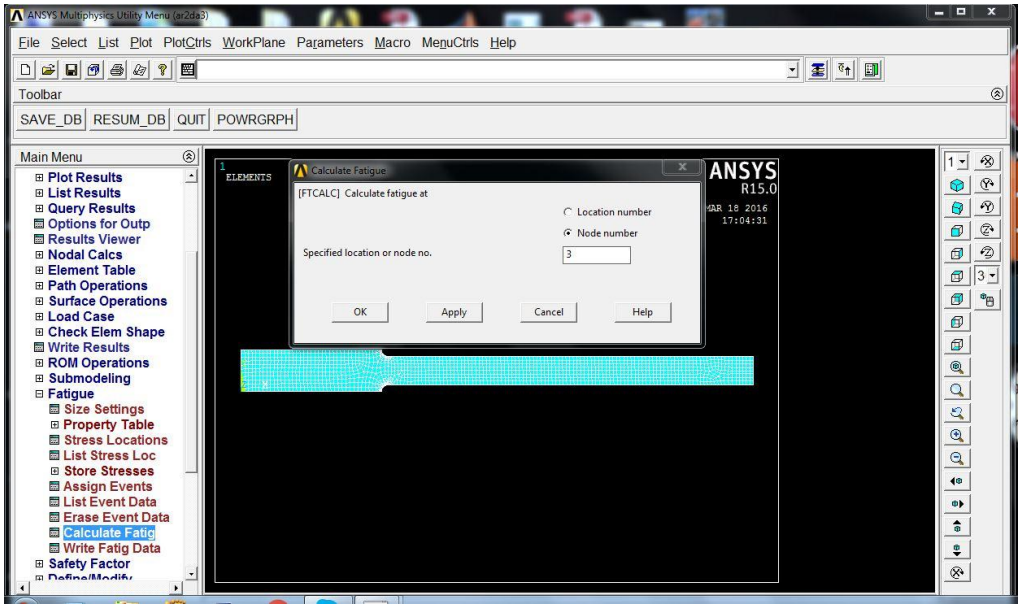

Fig. 2.30 Fatigue analysis for NLOC=1

The partial usage value, is the ratio of cycles used/cycles allowed. The Cumulative Fatigue Usage value is sum of the partial usage factors.

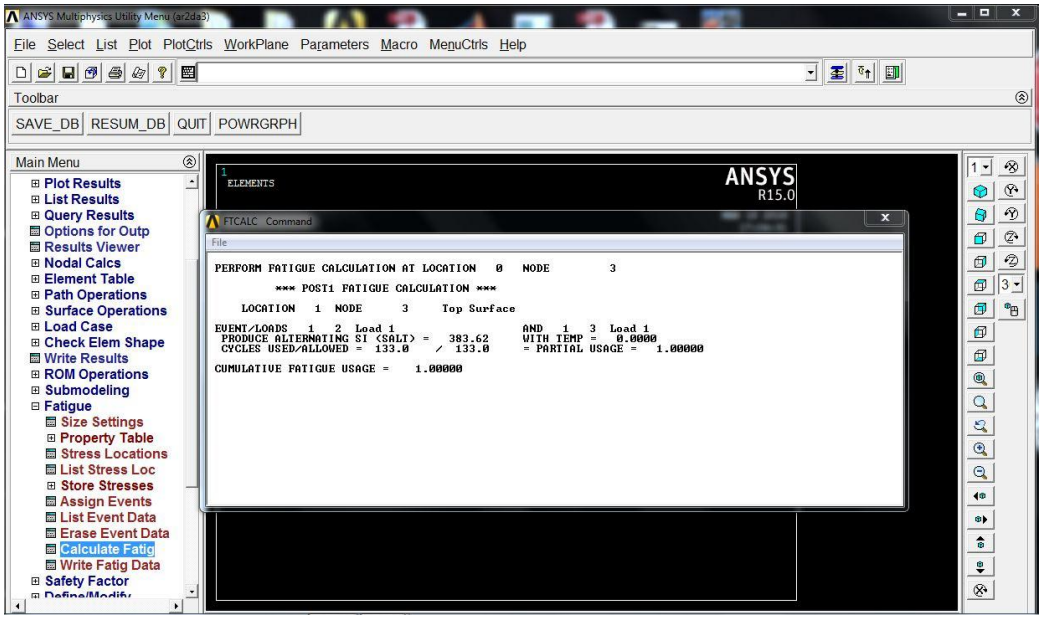

Fig. 2.31 Fatigue analysis result for NLOC=1

2.10 Conclusion

In the present chapter, methodology used for performing LCF analysis is discussed. The methods are mainly experimental, theoretical, empirical and numerical. Next chapter presents results obtained for LCF analysis of as received AA6063 alloys at room temperature condition using the above methodologies .